International Journal of the Physical Sciences Vol. 6(24), pp. 5738-5751, 16 October, 2011
Available online at http://www.academicjournals.org/IJPS
DOI: 10.5897/IJPS11.1061
ISSN 1992 - 1950 ©2011 Academic Journals

Full Length Research Paper

A GIS-based survey for the optimization of infiltration forecasting models with emphasis on slope effect and land use

Mohammad Dorofki[1]*, Ahmed H. Elshafie[1], Othman Jaafar[1], Othman A. Karim[1] and Sharifah Mastura Syed Abdullah[2]

[1]Department of Civil and Structural Engineering, Faculty of Engineering and Built Environment, UKM, Bandar baru bangi, Selangor, Malaysia.
[2]Faculty of Social Sciences and Humanities, UKM, Bandar baru bangi, Selangor, Malaysia.

Accepted 23 August, 2011

Morphology and specifically slope have an important effect on water losses due to infiltration and obtained runoff from rainfall. Approximately all of infiltration models survey infiltration in the large scale region (like a basin) and through a vertical column. In other words, they work with this assumption that slope is equal to zero. There are few infiltration models such as modified green and Ampt model which use the slope as an input factor. But, since this parameter is the average slope of whole catchment, it cannot be really accurate. This paper is a raster-based investigation of slope effect on infiltration by considering land use which is one of the most important parameters in this case. For this purpose, geographic information system (GIS) has been used to divide Johor river basin in the south of Malaysia to 1436200 separated pixels (10 × 10 m) and study on each pixel as an independent catchment. To corroborate the suitability of the obtained results, eighteen different type of slope has been studied. The correlation coefficient indicates that thesquare cosine of slope is the most suitable function of slope which can be used for infiltration calculations.

Key words: Malaysia, infiltration forecasting model, surface slope, geographic information system, land use, digital elevation model.

INTRODUCTION

Soil and water conservation is one of the most important objectives in natural resources management. Totally, three parameters are involved in this case: rainfall, runoff and percentage of water infiltrated into soil. The main principle of soil and water conservation is to increase infiltrating water and decrease volume and flow rate of surface runoff, then minimize soil degradation that can be caused by erosion. Infiltration is defined as the process by which a fluid passes through or into another substance travelling through pores and interstice. When raining, rainwater infiltrates into the subsurface soil through the unsaturated zone on the top (Muntohar and Liao, 2010).

*Corresponding author. E-mail: rezvan59rs@yahoo.com or dorofki@eng.ukm.my. Tel: +60-123490294.

In the analysis of flow through soils that are non-uniform with depth, it is often assumed that soil hydraulic properties are more homogeneous within horizons or layers than between layers (Beven, 1984). Water movement in soil can be described accurately at the local scale, provided that soil hydraulic properties can be determined with precision. Also, the estimation of infiltration is an extremely sensitive parameter, because a low runoff coefficient will underestimate the amount of sub-basin runoff while a high runoff coefficient will overestimate the amount of sub-basin runoff. So, it is extremely important to accurately estimate sub-basin runoff coefficients using the best data and most advanced computation methods available (Smemoe, 1999).

Infiltration models play an important role in water resource management planning and therefore, different types of models with various degrees of complexity have been developed for this purpose (El-shafie et al., 2011), because most of the methods for characterizing soil are often time consuming and work with this assumption that slope is equal to zero. Large areas cannot be sampled easily (Braud et al., 2005). There are two main approaches to describe the time dependent function of infiltration through a vertical column. Some are physically based (like Green-Ampt and Philip equations), derived from the interaction between soil hydrologic properties (Fernández-Gálvez et al., 2008) while others are empirically based (like Horton, Kostiakov and modified Kostiakov equations), composed from the results of experiments and statistical analysis (Sepaskhah and Chitsaz, 2004). Morphology parameters such as area, width, shape and specially slope effect on water losses due to infiltration and obtained runoff from rainfall (Jain and Singh, 2005). Previous studies have demonstrated the dominant influence of soil surface features over land flows (Casenave and Valentin, 1992) especially by determining the flow partitioning between infiltration and runoff. Nevertheless, there is lack of comprehensive researches which have investigated on the real effect of morphologic gradient during infiltration process in the local scale.

The hydrologic effect of land use changes have been thoroughly described (Calder, 1993). The major changes in land use that affect hydrology are afforestation and deforestation, the intensification of agriculture, the drainage of wetlands, road construction and urbanization Calder, 1993). Land use also influences the infiltration and soil water redistribution process, because saturated hydraulic conductivity is influenced by plant roots and pores resulting from soil fauna (De Roo et al., 2001). An extreme example is the influence of buildup areas and roads on overland flow. Hundecha and Bardossy (2004) analyzed effect of different type of land use on infiltration and calculated a coefficient factor for each kind of coverage.

Geographic information system (GIS)

Recent developments in geographic information system (GIS) techniques have enhanced the capabilities to handle large databases describing the heterogeneities in land surface characteristics (Jain et al., 2004). The digital elevation model (DEM) is one of the products of digital mapping technique which can automatically extract topographic variables, such as basin geometry, stream networks, slope, flow direction, etc., from raster data on elevation. Three schemes of structuring elevation data for DEMs are triangulated irregular networks (TIN), grid (pixel) networks and vector or contour based networks (Moore and Grayson, 1991). The most widely used data structure is the grid network. The grid or cell approach adapts well to the collection of input data on a regular pattern with the use of remote sensing and GIS and accounts for the variation in topographic characteristics within a catchment (Wigmosta et al., 1994). The grid-based discretization of catchment is also immensely useful for numerical solution of the partial differential equations governing the rainfall-runoff process (Abbott et al., 1986). Also, there are some of the distributed hydrological models that use grid or cell approach and are structured to derive the advantage of using data available in GIS format (Band et al., 1993; Grayson et al., 1992; Watson et al., 1998). These models are also capable of quantifying the effect on runoff of variability in physical characteristics of the catchment (Beven and Freer, 2001; Grayson et al., 1992). Comprehensive reviews on the past efforts and current trends in using DEMs and GIS to perform hydrological analyses are available in Moore (Moore et al., 1993), Vieux (Vieux, 2004), etc. GIS with its capability in analyzing phenomenon by raster format can allow users to separate a wide region to several smallish areas and calculate infiltration in each pixel separately by using DEM (Bastawesy et al., 2008). But digital methods have a number of limitations in defining a watershed, with the primary limitation being the vertical resolution of the DEM (French et al., 2006). Also, GIS assisted database system would help to apply groundwater management practices, such as proper groundwater resource management in terms of groundwater quality and quantity, integrated management of water, land use and environment (Ashraf et al., 2011).

As most hydrological parameters are subjected to the uncertainty, proper forecasting methods are of interest for experts to overcome the uncertainty (Othman and Naseri, 2011). The present study is araster-based approach to identify the actual effects of topography (specially slop) in the course of infiltration process in GIS environment by considering rainfall, land use and surface slope of self-governing pixels within the basin as independent catchments.

MATERIALS AND METHODS

Data preparation and database making

Infiltration is one of the most important issues to the recognition of the relation between rainfall and runoff for a watershed (El-Shafie and Seyed, 2011). Our model uses the total volume of rainfall excess which accumulates in topographic depressions in the study area. This volume of rainfall excess (total volume of rainfall is neither obtained runoff nor returned to the atmosphere as evaporation or transpiration, in) is determined by Equation 1 using the mass balance equation.

$$I = R - F - E - T \quad (1)$$

where I is infiltration rate (rainfall excess), R is rainfall intensity, F is the obtained runoff, E is evaporation and T is transpiration (all in m^3/s). Evaporation (E) and transpiration (T) were not incorporated in our model, because the amount of these two parameters in per unit area in the tropical environment is very low (Calder et al., 1986). Seasonality effects (like temperature and humidity) can also be ignored, while the study area discussed in this research is located in the low latitudes (next to the equator) and there are no different circumstances (seasons) in these kinds of areas.

Based on current data availability and exciting stations in Johor basin, Pengeli catchment (Figure 2) was selected as a case study. Rainfall and runoff data can be collected from historic rainfall data available through the Department of Irrigation and Drainage Malaysia (JPS), for the nearest stations. In this case, weekly rainfall data (R_w) of the five stations (Tables 2 and 3) and observed weekly runoff data (F_w) of the one station (Table 4) as an outlet have been used for ten years. For this purpose, Theissen polygons (Figure 4) have been created to specify the boundary of effectiveness of each station (Figure 5) by use of coordinates of the five specified rainfall stations. As Pengeli basin is located in a tropical region and fluctuations of rainfall in these areas is independent from height changes, then Theissen polygons are the best method for rainfall interpolation. After that, DEM (Figure 6), slope map (Figure 7) and land use map (Figure 8) were developed by conversion of shape file maps to raster format in GIS environment, for each five of the regions.

In a raster-based GIS, the flow domain (catchment) was divided into an array of grid or cells, each of which represents an area with average properties. In this study selected pixel resolution is given by 10 × 10 m. The researched selected region is having a significant number of 1436200 (Table 5) and each of them has an area of 100 m^2. In hydrologic terms, when infiltration is focused and discussed, the different independent pixels can be taken under research. By making the working unit smaller, the outcome of the research becomes more accurate, since the involved parameters in infiltration are mostly affected in the vertical direction. For this reason, one comprehensive database including coordinates, slope (S%), land use factor (γ_i, which is 40.38% for forest and 43.77% in agricultural regions (Hundecha and Bardossy, 2004)) and the weekly average rainfall and runoff data was prepared for each pixel by sampling. To process the runoff data first of all, the unique hydrograph was calculated and then the amount of it (0.5) was deducted from the actual runoff data. By decreasing weekly output amount of basin's runoff from the total amount of weekly rainfall (Equation 1) the infiltration rate (Table 6) could be calculated during the discussed period of time. Weekly infiltration amount (I_c) was also added in the information chart for each pixel in the database. Based on the given data, to acquire the real effect of slope on infiltration, inverse of slope ($\frac{1}{s}$), slope square (S^2), inverse of slope square ($\frac{1}{s^2}$), slope root square ($\sqrt{s}$), inverse of slope root square ($\frac{1}{\sqrt{s}}$), SINE of slope ($\sin s$), inverse sine of slope ($\frac{1}{\sin s}$), sine square of slope ($\sin^2 s$), inverse sine square of slope ($\frac{1}{\sin^2 s}$), sine root square of slope ($\sqrt{\sin s}$), inverse root square sine of slope ($\frac{1}{\sqrt{\sin s}}$), cosine of slope ($\cos s$),inverse cosine of slope ($\frac{1}{\cos s}$),cosine square of slope ($\cos^2 s$), inverse cosine square of slope ($\frac{1}{\cos^2 s}$), cosine root square of slope ($\sqrt{\cos s}$) and inverse root square cosine of slope ($\frac{1}{\sqrt{\cos s}}$) beside the slope (s) were imported for completion of the database as slope factor of the each pixel (μ_i). In the end, the rainfall amount of each pixel (R_w) was multiplied into Slop factor of the each pixel (μ_i) by considering land use factor (γ_i) and then, the amount of infiltration (I_c) is reduced from the calculated number (Equation 2) to estimate the pixel's runoff index (F_c). In other words, instead of using the average of basin's slope, the effect of the differed types of the slope is preferred in each 100 m^2. It should be noted that, as 97% of Pengeli basin is covered by agriculture and forest (Figure 8), other covers have been ignored.

$$F_c = [\sum((R_w * \mu_i)\gamma_i)] - I_c \quad (2)$$

where F_c in m^3 is calculated runoff index, R_w in m^3 is weekly rainfall, μ_i is Slop factor of the each pixel, γ_i is land use factor of the each pixel and I_c in m^3 is calculated infiltration.

Statistical analysis

Correlation and dependence are any of a broad class of statistical relationships between two or more random variables or observed data values. Correlations are useful, because they can indicate a predictive relationship that can be exploited in practice. Formally, dependence refers to any situation in which random variables do not satisfy a mathematical condition of probabilistic independence. In general statistical usage, correlation or co-relation can refer to any departure of two or more random variables from independence, but most commonly refers to a more specialized type of relationship between mean values.

The correlation coefficient was used to inspect the correlation between the actual runoff data and the complex of calculated data (Figure 3). Subsequently, in conclusion, correlation is calculated between the observed weekly runoff data (F_w) and calculated weekly runoff index (F_c) separately for 10 years.

Study area

Malaysia is a developing country that moves towards the vision 2020. Johor river basin (Figure 1) is one of the largest catchment in south of Malaysia with an area of 2751.72 km^2 and is located between the 1° 27′ N to 1° 49′ N latitudes and 103° 42′ N to 104°01′ N longitudes. Johor river considers the main river in Johor basin (Table 1). The river flows in a roughly north-south direction and empties into the Johor.

Johor has a tropical rainforest climate with monsoon rain from November until February blowing from the South China sea. The average annual rainfall is 2,470 mm with average temperatures ranging between 25.5 °C (78 °F) and 27.8 °C (82 °F). Humidity is between 82 and 86%. The highest point in Johor basin is Gunung Ledang (1276 m). Johor also has a 400 km coastline on both the East and the West coasts. On 19 December 2006, a continuous heavy downpour occurred in Johor, which led to the 2006 to 2007 Malaysian floods. Many towns such as Muar, Kota Tinggi and Segamat were seriously flooded with water levels as high as 10 feet (3.0 m) above ground level recorded in some areas.

RESULTS AND DISCUSSION

There are three different situations in the term of infiltration process regarding rainfall intensity:

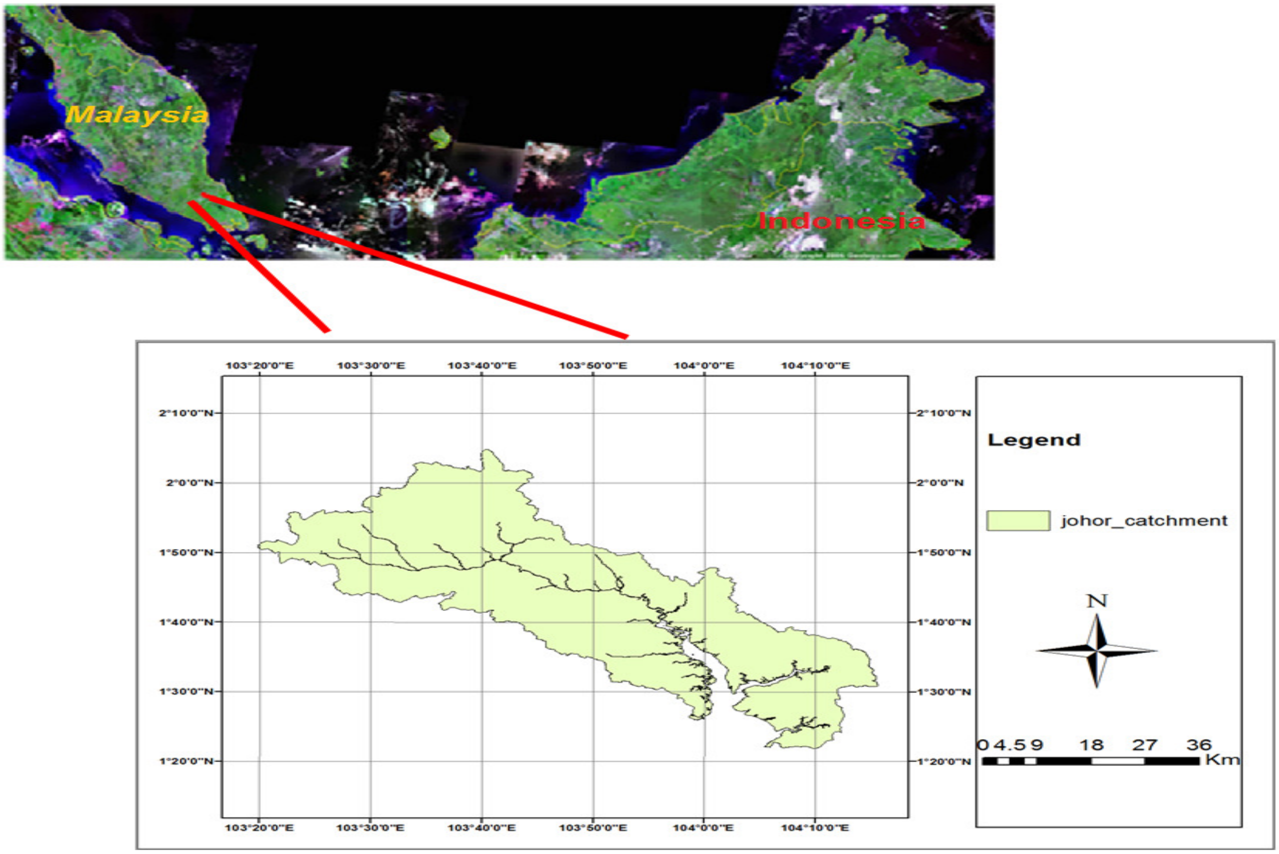

Figure 1. J ohor river basin (study area location) in the south of Malaysia.

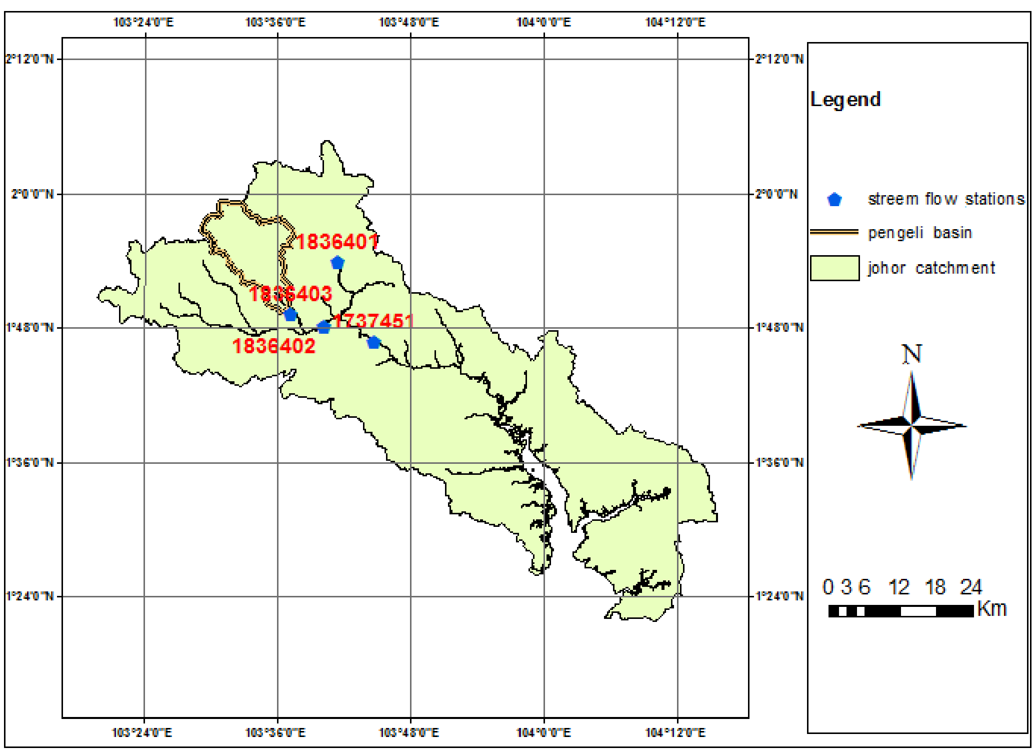

Figure 2. Pengeli basin and its outlet (runoff stations number: 1836403).

Table 1. Johor river basin characteristics.

Location: Central part of south Johor	N 1° 27′ – 1° 49′	E 103° 42′ – 104° 01′
Area: 2751.72 km2	**Length of main stream:** 122.7 km	
Origin: Mountain Gemuruh (109 m)	**Highest point:** Mountain Belumut (**1.010 m)**	
Outlet: Stairs of Johor	**Lowest point:** River Mouth (0 m)	
Main geological features: Intrusive rocks, Quaternary, Triassic, Permian, Cretaceous-Jurassic, Tertiary		
Main tributaries: Pengeli river, Sayong river, Linggui river, Semangar river, Tiram river, Layang river		
Main lake: Nil		
Main reservoirs: Linggui Dam (impounded in 1993)		
Mean annual precipitation: 2.470 mm (basin average)		
Mean annual runoff: 37.5 m^3/s		
Population: 220,000	**Main city:** Kota Tinggi	
Land use: Urban (5.5%), forest (16.4%), oil palm and other crops (18.5%), waterbody (0.5%), swamps (11.6%)		

Table 2. Average of annual rainfall (mm) in 5 stations which have been chosen for rainfall interpolation in Pengeli basin.

Station / Year	1835001	1836001	1834001	1834122	2034001	Average of years
1989	40.00	40.10	32.30	30.80	39.06	36.452
1990	55.97	37.21	30.13	43.86	41.01	41.636
1999	50.51	39.22	40.96	41.08	43.60	43.074
2000	50.60	43.09	43.89	38.48	44.86	44.184
2001	46.32	31.60	39.46	33.49	36.17	37.408
2002	56.37	44.87	40.76	38.58	38.22	43.76
2003	48.00	49.47	37.42	39.74	40.20	42.966
2004	44.02	52.50	43.93	44.02	52.63	47.42
2005	41.92	42.85	18.37	41.44	36.21	36.158
2006	69.17	59.24	44.73	45.61	52.11	54.172
Total average	50.288	44.015	37.195	39.71	42.407	42.723

Table 3. Maximum of annual rainfall (mm) in 5 stations which have been chosen for rainfall interpolation in Pengeli basin.

Station / Year	1835001	1836001	1834001	1834122	2034001
1989	126.00	191.50	128.50	148.50	179.50
1990	462.50	168.50	138.00	199.50	221.50
1999	237.50	202.00	188.30	136.00	194.50
2000	171.50	216.00	176.90	127.00	157.00
2001	225.00	160.00	164.80	92.00	193.00
2002	294.00	247.00	159.30	204.00	202.00
2003	182.00	164.00	127.90	132.00	193.00
2004	251.00	328.50	389.00	330.00	294.00
2005	188.00	141.00	110.90	156.50	179.00
2006	365.00	398.00	441.00	327.00	460.00

1. Rainfall intensity is larger than infiltration rate. Ground surface becomes saturated in the entire time interval. Hence, surface slope does not have a large effect in this kind of situation.

2. Rainfall intensity is smaller than the infiltration rate at the beginning of the time interval, but becomes larger than the infiltration rate later. So, the ground surface changes from unsaturated to saturated condition in this

Table 4. Average, maximum and minimum of runoff (m^3/s) in each year in the outlet in Pengeli basin (Station number: 1835403).

Year	1989	1990	1999	2000	2001	2002	2003	2004	2005	2006
Average	2.45	3.89	4.86	4.94	4.89	8.36	3.12	4.51	3.21	2.09
Maximum	6.71	22.61	17.52	12.48	24.04	29.91	10.17	17.05	14.65	6.02
Minimum	0.49	0.98	2.27	2.55	1.44	0.42	1.54	0.61	0.52	0.37

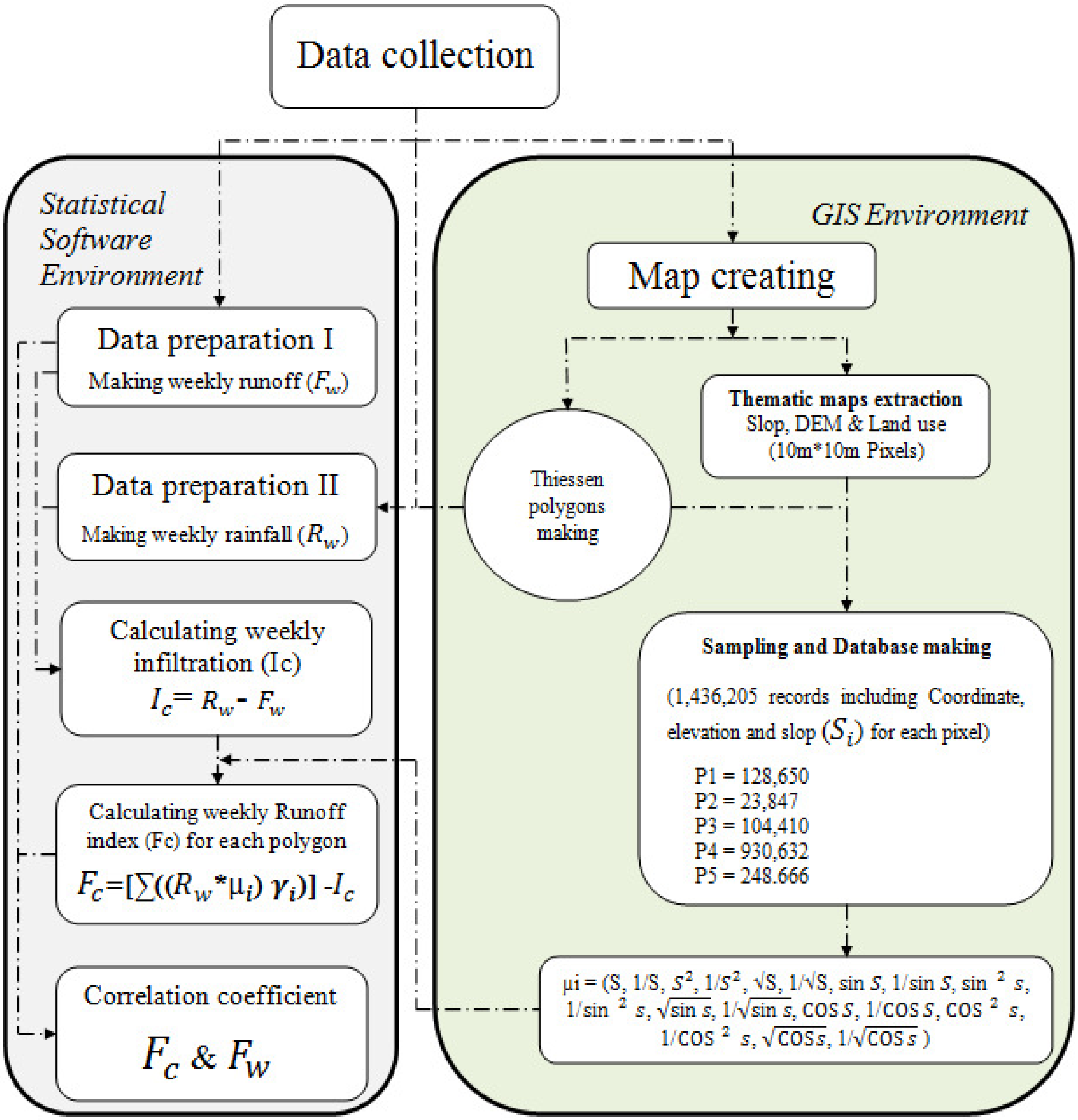

Figure 3. Schematic representation of the research (Application of GIS to extract the necessary information of each pixel in a raster-based environment).

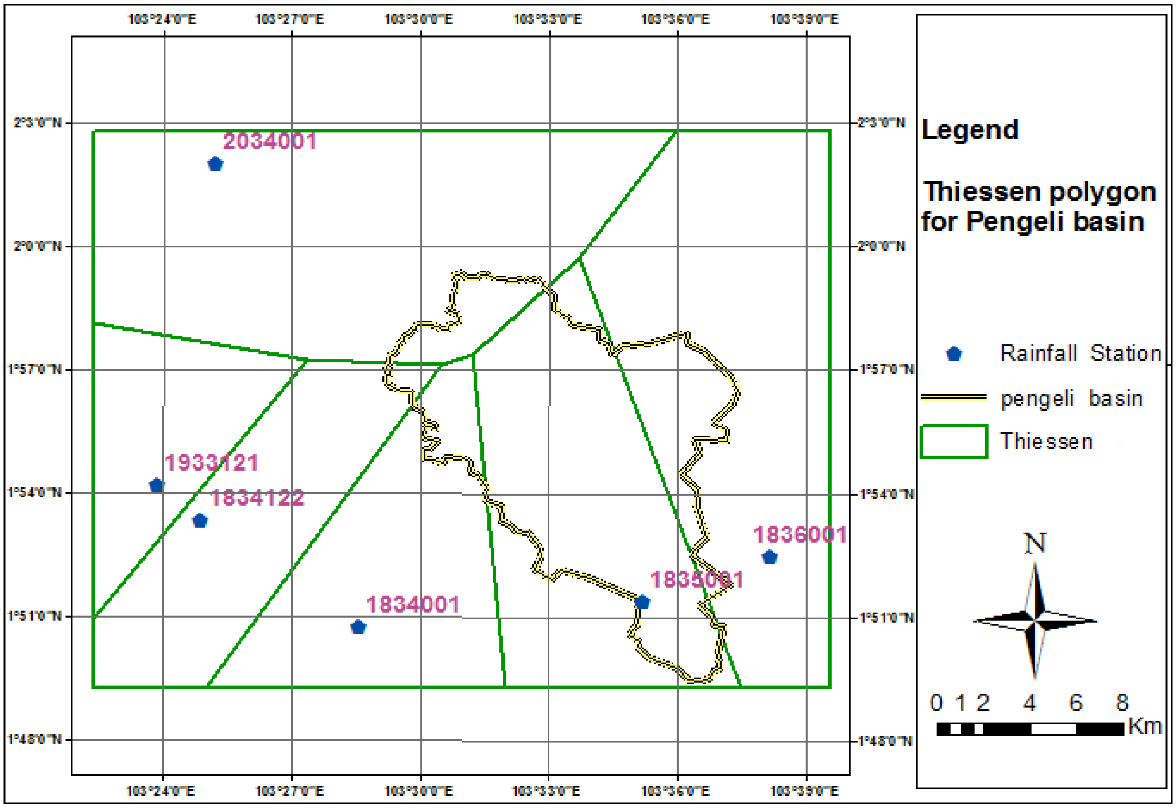

Figure 4. Thiessen polygons making for rainfall interpolation in Pengeli basin.

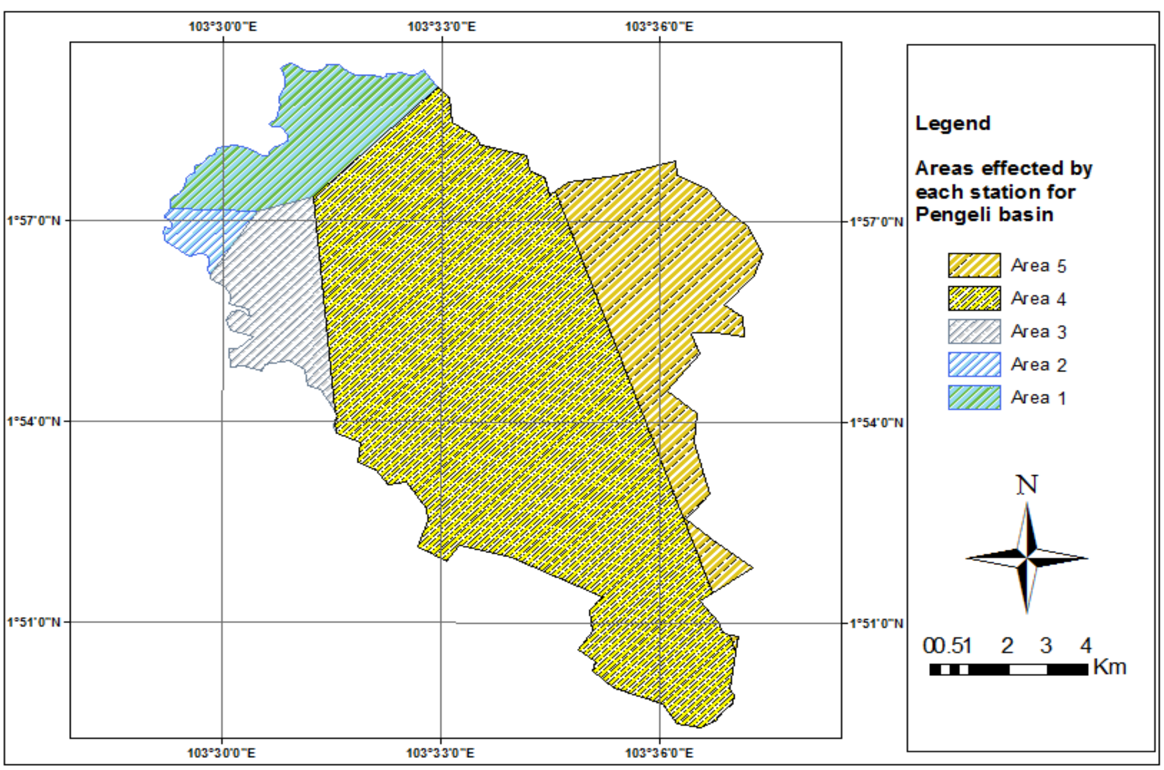

Figure 5. Effected area by each rainfall station after applying Thiessen polygonsin Pengeli basin (Table 5).

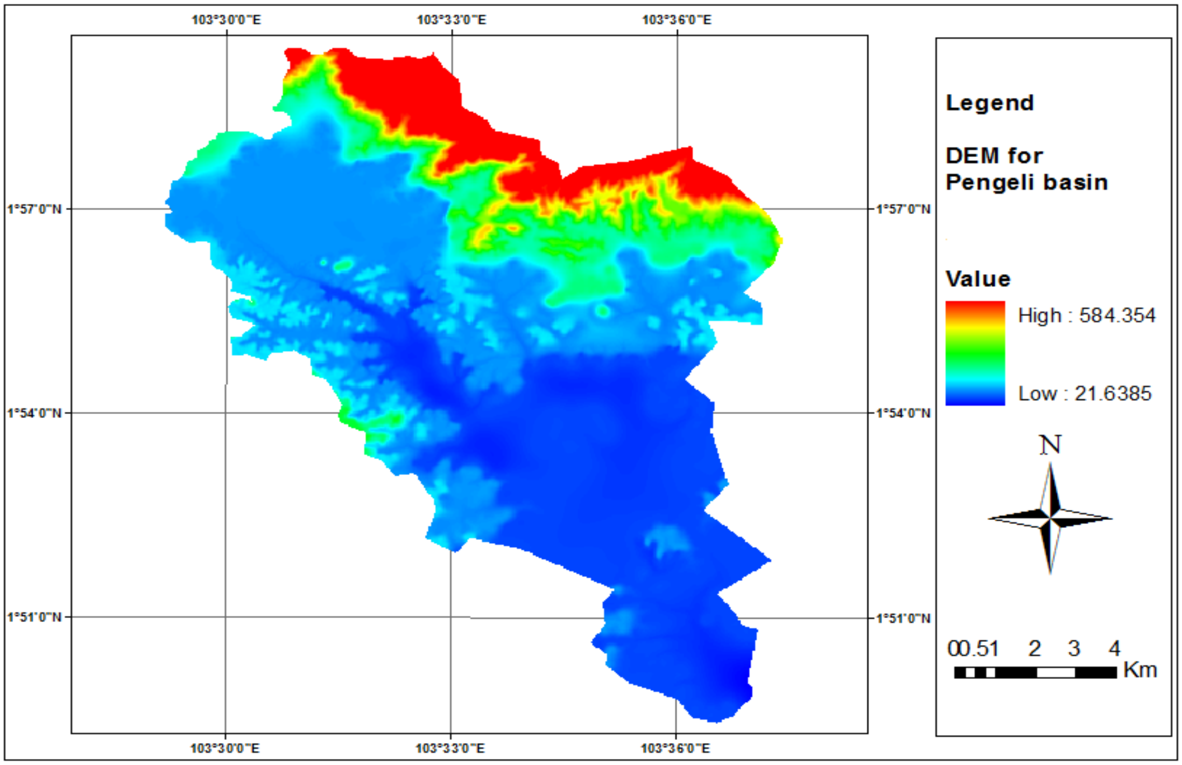

Figure 6. Creating 10×10m DEM (Digital Elavation Model) to extract slope map.

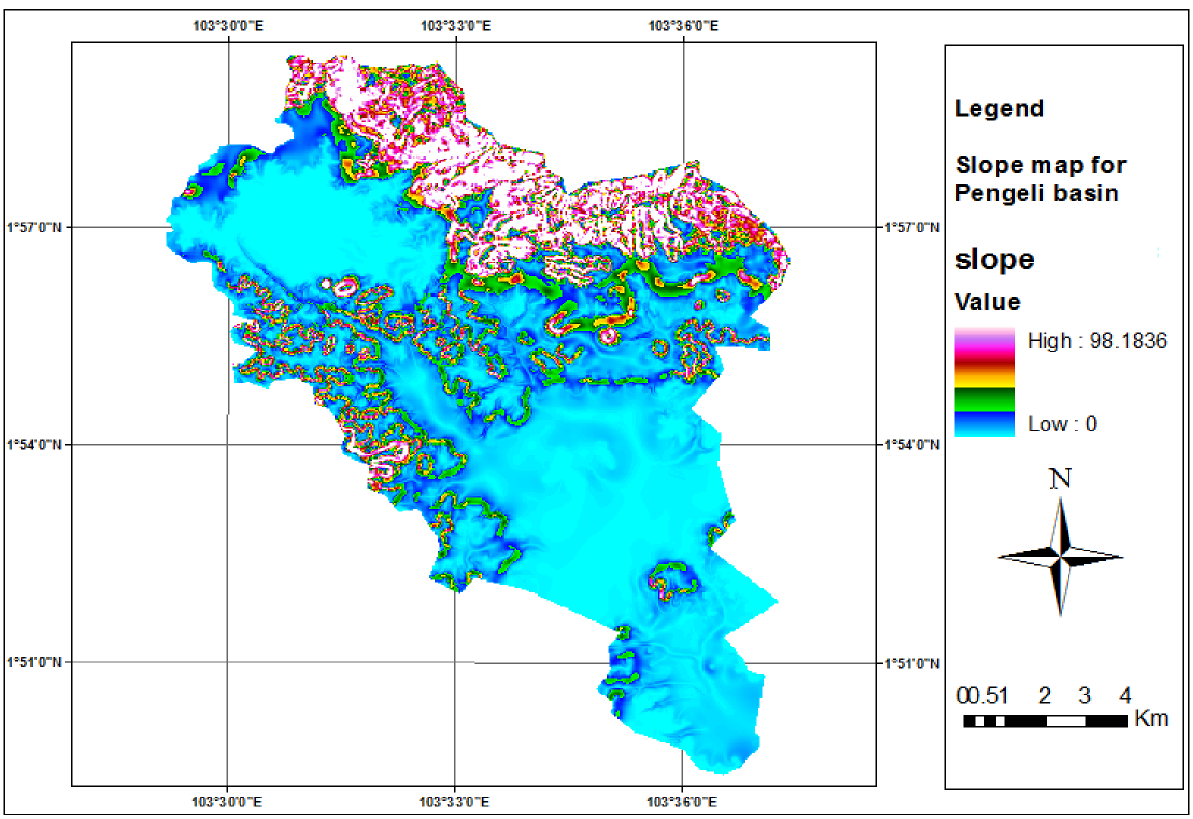

Figure 7. Slope map of Pengeli basin (contain of slope for each 10 ×10m pixel).

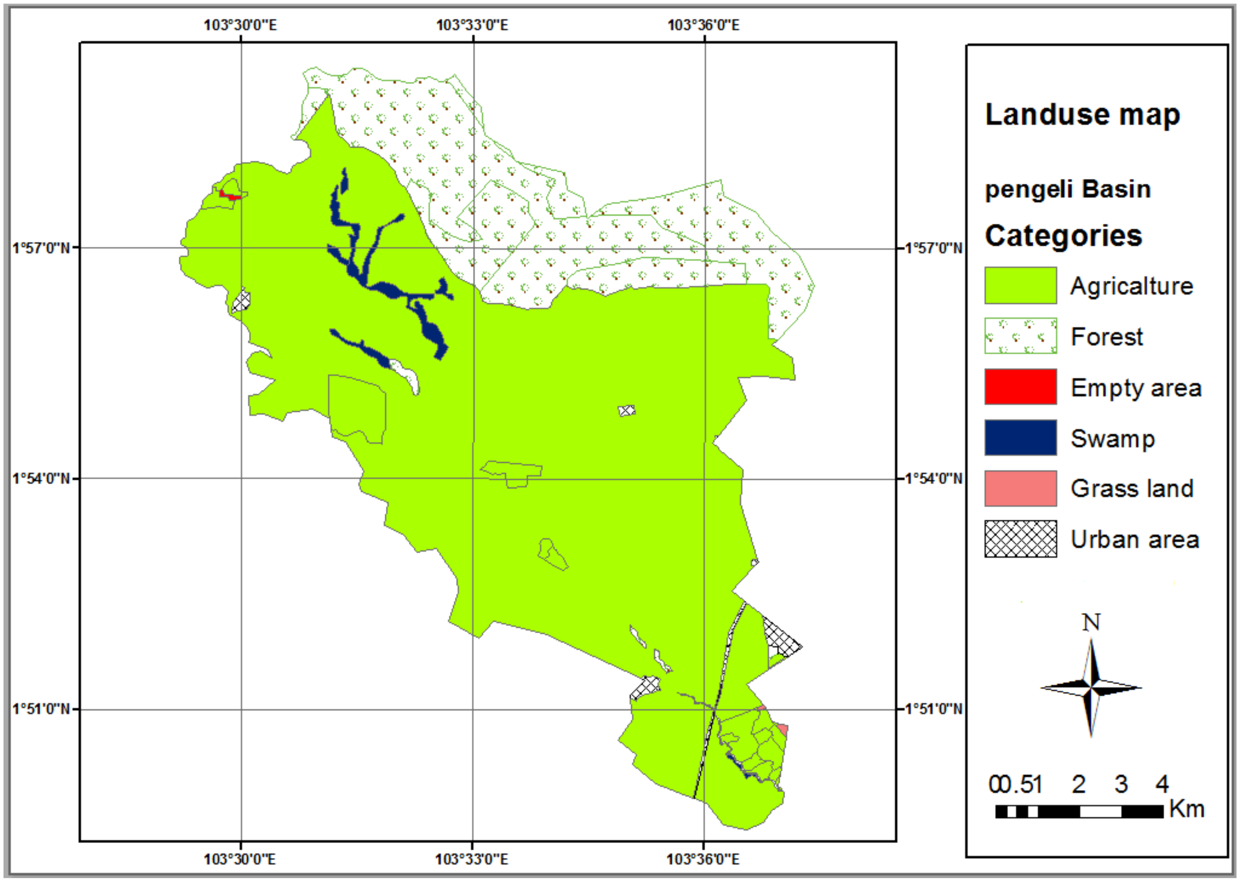

Figure 8. Land use map of Pengeli basin (97% covered by agriculture and forest).

Table 5. Characteristics of different regions that are affected by each rainfall station after applying Thiessen polygons interpolation in Pengeli basin (Figure 4).

Station	Number of pixels	Area (Acer)	Slop (100%)	Elevation (m)
2034001	128649	3177.63	16.57	180.00
1834122	23873	589.66	1.59	62.08
1834001	104409	2578.90	6.39	65.91
1835001	930631	22986.59	8.09	79.64
1836001	248638	6141.36	13.15	121.64
Sum/Average	Sum = 1436200	Sum = 35474.14	Average = 9.5	Average = 94.61

Table 6. Calculated I_c (infiltration rate) for Pengeli basin in each year (mm/s).

Year	1989	1990	1999	2000	2001	2002	2003	2004	2005	2006
I_c	0.00271	0.00317	0.00274	0.00256	0.0022	0.00277	0.00317	0.00271	0.00269	0.00496

time interval. It means that gradient slope will cooperate as a main parameter during infiltration progression.

3. Rainfall intensity is smaller than infiltration rate during the time interval. Under this condition, surface is not saturated and all the rainfall infiltrates into soil. Then, the rate infiltration is equal to the rainfall intensity, and it will proceed independent from slope.

Land use also affects the infiltration rate by impress saturated hydraulic conductivity of the soil. Forests have a higher potential of hydraulic conductivity as compared

Table 7. Correlation coefficients between F_w (observed weekly runoff) and F_c (observed runoff index) for each function.

-	Function	R^2	-	Function	R^2
1	R*S	0.3102	10	R/$\sin^2 s$	0.2399
2	R/S	0.2525	11	R*$\sqrt{\sin s}$	0.0952
3	R*S^2	0.4252	12	R/$\sqrt{\sin s}$	0.3014
4	R/S^2	0.1194	13	R*$\cos S$	0.8513
5	R*$\sqrt{S}$	0.2841	14	R/$\cos S$	0.7681
6	R/$\sqrt{S}$	0.2494	15	R*$\cos^2 s$	0.8527
7	R*$\sin S$	0.0154	16	R/$\cos^2 s$	0.7401
8	R/$\sin S$	0.2538	17	R*$\sqrt{\cos s}$	0.8481
9	R*$\sin^2 s$	0.0061	18	R/$\sqrt{\cos s}$	0.7790

Table 8. Classification of different functions of slope (18 functions) via obtained correlation coefficient (cosine functions show the highest correlation).

Functions	Range of correlation coefficient (%)	Qualitative correlation
$\sin s$ (3 functions)	CC ≈ 0	Without correlation
$\csc s$ ($\frac{1}{\sin s}$) (3 functions)	23 < CC < 30	Low correlation
Normal (6 functions)	11 < CC < 42	Average correlation
$\sec s$ ($\frac{1}{\cos s}$) (3 functions)	74 < CC < 77	Relatively high correlation
$\cos s$ (3 functions)	84 < CC < 86	High correlation

to the agricultural fields, which are two main coverage of land use in the current study area. Therefore, infiltration rate increases with increasing areas of forest and decreasing areas of agriculture. The current forests within the catchment are largely concentrated in the steep land areas in the upstream of the catchment (Figures 7 and 8). So, these forests are not able to increase the infiltration rate of the catchment due to the high slope in districts.

According to the achieved results and correlation coefficients (Table 7), relation between the slope and discharge (and consequently infiltration) could be categorized into five categories which have been shown in Table 8, respectively.

As it has been shown in Table 8 the highest obtained correlation coefficient is 85%. This can be considered as a logic amount because it is between observed runoff data (F_w) and calculated runoff index (F_c). This calculated runoff index has been obtained by multiplying actual rainfall data (R_w) and each slope function (by considering land use factor for each pixel), minus infiltration (I_c) which the procedure is shown in Figure 3, correspondingly. On the other hand, this highest correlation has been obtained by cosine functions (Figure 9). This could be expected based on Newton's law of motion. Principally, the effect of sinusoidal force (F* $\sin \alpha$) is being neutralized by the surface reaction. This force can have an effect on friction motion and not on the subject's movement. Therefore, sinusoidal functions show low correlation; because the desired ambulatory object (water) is fluid and fluid objects do not produce high friction. While, cosine force (F* $\cos \alpha$) has straight effect on the ponding depth. In addition, the cosine determines the amount of water on a gradient surface unit which is different from other flat surface units. This amount of water on the surface unit has a direct relation with infiltration amount (Figure 10). This study, the best results of cosine as horizontal distance (unlike sinus which means vertical distance or height) between two point in a ramp, has been shown.

Beside, since the average slope (9.5%) of the basin is low (Table 5) thus, there is not much difference between those factors which are in the same category (Table 8). This theme is obvious in trigonometric functions specially, because when sine and cosine are taken from small numbers, the results will be close to each other, but results of square cosine functions in different years (Table 9) specify that this function is the most suitable function for slope to use as a parameter in infiltration forecasting models.

Finally, according to achieved correlation coefficient for each function in different years (Figure 11), this can address that there is a reverse relationship between mean rainfall (Table 2) and correlation coefficient in each year. Hence, there is low correlation coefficient when the

Table 9. Correlation coefficient of each function in each year.

Function \ Year	1989	1990	1999	2000	2001	2002	2003	2004	2005	2006
R*S	0.3726	0.5661	0.6658	0.8551	0.6950	0.1830	0.3230	0.5403	0.2468	0.2553
R/S	0.5325	0.4837	0.6559	0.5494	0.5916	0.0777	0.3556	0.5644	0.2435	0.1354
R*S^2	0.4450	0.6477	0.7525	0.8901	0.7753	0.3852	0.3772	0.6268	0.3627	0.2915
R/S^2	0.6145	0.6591	0.7657	0.7737	0.7089	0.3815	0.4308	0.6449	0.4213	0.0855
R*$\sqrt{S}$	0.3536	0.5468	0.6430	0.8455	0.6746	0.1348	0.3100	0.5179	0.2207	0.2526
R/$\sqrt{S}$	0.5259	0.4763	0.6536	0.5375	0.5903	0.0742	0.3510	0.5648	0.2456	0.1404
R*$\sin S$	0.2063	0.2840	0.3121	0.6826	0.3030	0.4106	0.1833	0.2014	0.1023	0.2312
R/$\sin S$	0.5319	0.4841	0.6554	0.5513	0.5912	0.0752	0.3552	0.5638	0.2417	0.1339
R*$\sin S$	0.2220	0.3106	0.3504	0.7040	0.3474	0.3700	0.1961	0.2373	0.0722	0.1872
R/$\sin^2 s$	0.5259	0.5398	0.6536	0.5375	0.5903	0.0742	0.3510	0.5620	0.2488	0.1404
R*$\sqrt{\sin s}$	0.1654	0.2170	0.2123	0.6250	0.1859	0.4994	0.1510	0.1123	0.1713	0.1659
R/$\sqrt{\sin s}$	0.5197	0.5693	0.6880	0.7532	0.6475	0.1283	0.3659	0.5727	0.2555	0.0209
R*$\cos S$	0.9020	0.9286	0.9841	0.9851	0.9757	0.8130	0.7553	0.9096	0.8320	0.8478
R/$\cos S$	0.8781	0.9149	0.9755	0.9840	0.9623	0.7888	0.7120	0.8911	0.5096	0.8084
R*$\cos^2 s$	0.8776	0.9242	0.9815	0.9808	0.9776	0.8190	0.7450	0.9099	0.8428	0.6759
R/$\cos^2 s$	0.8070	0.8846	0.9562	0.9751	0.9441	0.7586	0.6479	0.8642	0.5024	0.6247
R*$\sqrt{\cos s}$	0.9062	0.9285	0.9840	0.9862	0.9738	0.8088	0.7531	0.9076	0.8239	0.9059
R/$\sqrt{\cos s}$	0.8965	0.9220	0.9800	0.9857	0.9673	0.7971	0.7316	0.8987	0.5110	0.8802

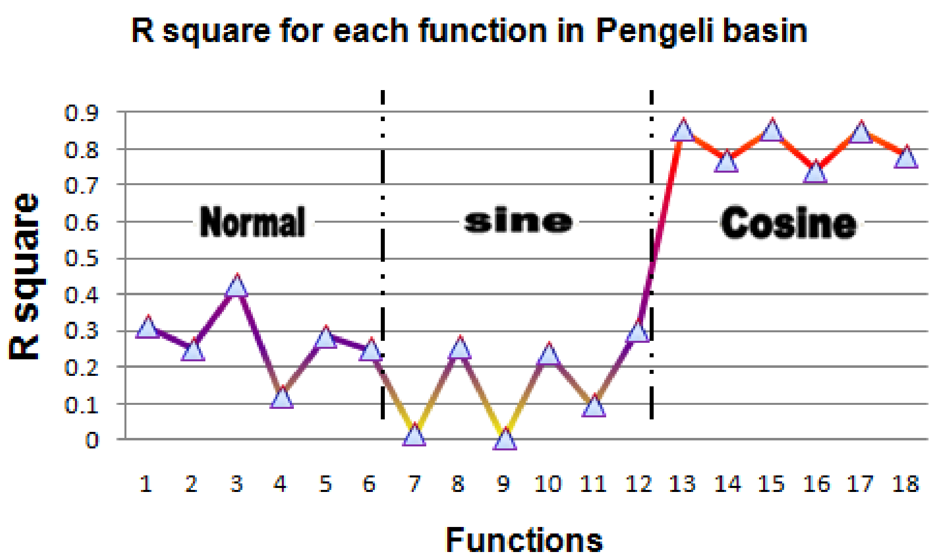

Figure 9. R square between F_w and F_c using 18 differentslope functions (each number in X-axis refers to a function regarding Table 7).

average of rainfall is high. It can be an evidence for this issue that infiltration parameters like soil properties and topology which is almost more effective when the rainfall has been started. Similarly, these parameters will lose their significance, decreasing by the factor of time. Thus, more rainfall will transform to the runoff since saturation of soil surface layers. This event happens when rainfall duration is long.

Conclusion

1. Since output of this paper is one percentage of runoff (F_c = Calculated runoff index, not calculated runoff). It is necessary to do further researches to calculate a correction coefficient for converting this calculated runoff index (F_c) to actual calculated runoff. Naturally, it will

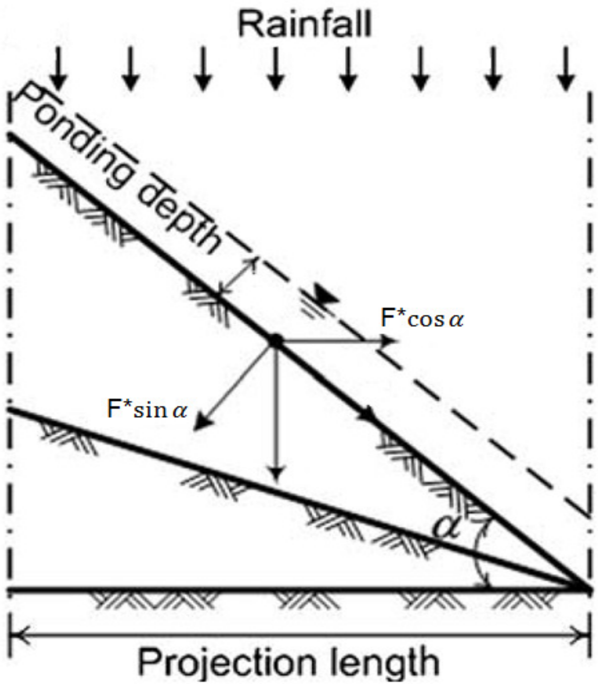

Figure 10. Newton's low of motion and its effect on sinusoidal and cosine forces.

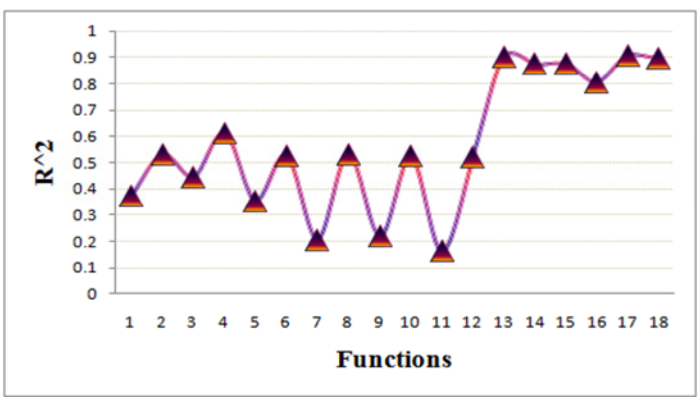

1989

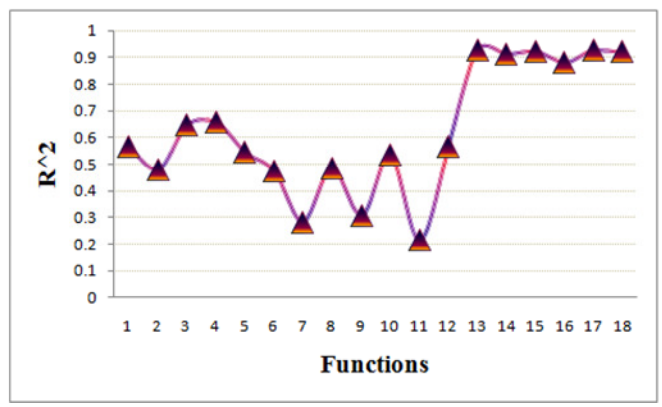

1990

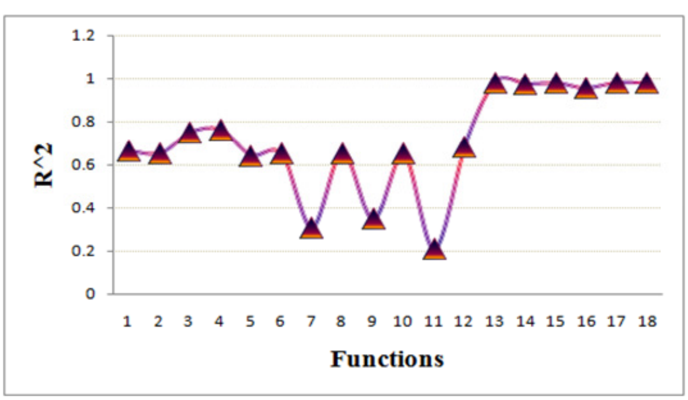

1999

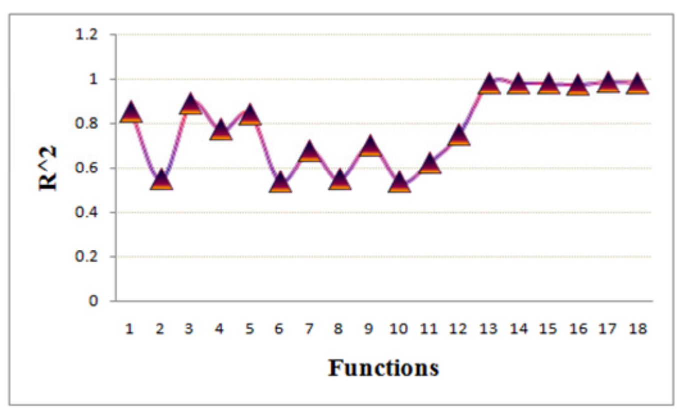

2000

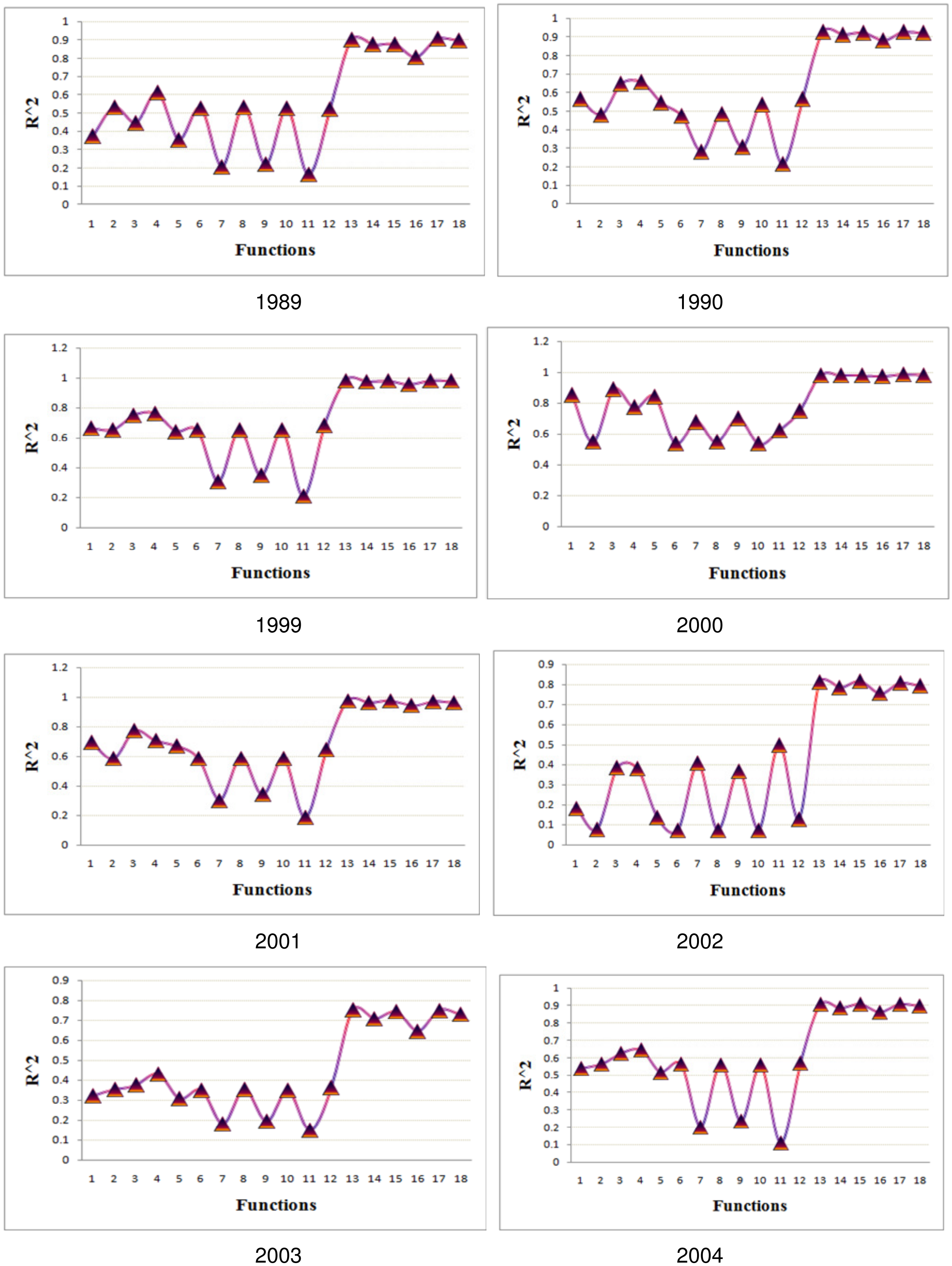

Figure 11. R square of each function in each year.

improve the current obtained correlation coefficient.

2. Forcefully, it is suggested to do the same researches in the catchments with different slopes and areas for comparing results. Outputs of this paper have been shown that basins with dissimilar morphology will have different correction coefficients.

3. Current study has prepared in a tropical and near to the equator area with a dominant land use of agriculture and forest (97%). Results indicate that identical studies on basins located in higher latitudes and different climates which effect on evaporation and transpiration are necessary. Divergent land use (such as urban areas) can be discussed regarding to the artificial surface phenomenon effects which will create more runoff due to the low infiltration potential.

4. Also, it is recommended that the obtained results scrutinize in different time series of infiltration (start, middle and the end) and, where the basins have different average rainfall.

ACKNOWLEDGEMENTS

This paper was prepared with financial support from the University Kebangsasan Malaysia (Project no. UKM-GUP-PLW-08-13-308): “Artificial Intelligence Model for River Inflow Forecasting”. We would also like to thank Department of Irrigation and Drainage Malaysia (JPS) for documentary data about rainfall and runoff.

Nomenclature: **I,** Infiltration rate (rainfall excess); I_c**,** calculated infiltration; R, rainfall intensity; R_w**,** weekly rainfall; **F,** obtained runoff; F_w**,** observed weekly runoff; F_c**,** calculated runoff index; **E,** evaporation; **T,** transpiration; S_i**,** Slop of the each pixel; μ_i**,** Slop factor of the each pixel; γ_i**,** land use factor of the each pixel.

REFERENCES

Abbott MB, Bathurst JC, Cunge JA, O'Connell PE, Rasmussen J (1986). An introduction to the European Hydrological System—Systeme Hydrologique Europeen. J. Hydrol., 87(1-2): 45-59.

Ashraf S, Afshari H, Ebadi AG (2011). Application of GIS for determination of groundwater quality suitable in crops influenced by irrigation water in the Damghan region of Iran. Int. J. Phys. Sci., 6(4): 843-854.

Band LE, Patterson P, Nemani R (1993). Running SW, Forest ecosystem processes at the watershed scale: incorporating hill slope hydrology. Agric. Forest Meteo., 63(1-2): 93-126.

Bastawesy MA, Khalaf FI, Arafat SM (2008). The use of remote sensing and GIS for the estimation of water loss from Tushka lakes, southwestern desert, Egypt. J. Afric. Earth Sci., 52(3): 73-80.

Beven K (1984). Infiltration into a class of vertically non-uniform soils. Hydrol. Sci. J., 29(4): 425-434.

Beven K, Freer J (2011). A dynamic top model. Hydrol. proc., 15(10): 1993-2011.

Braud I, De Condappa D, Soria JM (2005). Haverkamp R, Angulo-Jaramillo R, Galle S, Vauclin M, Use of scaled forms of the infiltration equation for the estimation of unsaturated soil hydraulic properties (the Beerkan method). Europ. J. Soil Sci., 56(3): 361-374.

Calder IR (1993). Hydrologic effects of land-use change. Chapter 13 in Maidment, DR, Handbook of Hydrol. McGraw-Hill, NY. p. 50.

Calder IR, Wright IR, Murdiyarso D (1986). A study of evaporation from tropical rain forest--West Java. J. Hydrol., 89(1-2): 13-31.

Casenave A, Valentin C (1992). A runoff capability classification system based on surface features criteria in semi-arid areas of West Africa. J. Hydrol., 130(1-4): 231-249.

De Roo A, Odijk M, Schmuck G, Koster E, Lucieer A (2001). Assessing the effects of land use changes on floods in the Meuse and Oder catchment. Phys. and Chem. of the Earth, Part B: Hydrol. Oceans. Atmos., 26(7-8): 593-599.

El-shafie A, Mukhlisin M, Najah AA, Taha MR (2011). Performance of artificial neural network and regression techniques for rainfall-runoff prediction. Int. J. Phys. Sci., 6(8): 1997-2003.

El-Shafie A, Seyed OJA (2011). Adaptive neuro-fuzzy inference system based model for rainfall forecasting in Klang River, Malaysia. Int. J. Phys. Sci., 6(12): 2875-2888.

Fernández-Gálvez J, Barahona E, Mingorance M (2008). Measurement of Infiltration in Small Field Plots by a Portable Rainfall Simulator: Application to Trace-Element Mobility. Water, Air, Soil Pollut., 191(1): 257-264.

French RH, Miller JJ, Dettling C, Carr JR (2006). Use of remotely sensed data to estimate the flow of water to a playa lake. J. Hydrol., 325(1-4): 67-81.

Grayson RB, Moore ID, McMahon TA (1992). Physically based hydrologic modeling 1.A terrain-based model for investigative purposes. Water Resour. Res., 28(10): 2639-2658.

Hundecha Y, Bardossy A (2004). Modeling of the effect of land use changes on the runoff generation of a river basin through parameter regionalization of a watershed model. J. Hydrol., 292(1-4): 281-295.

Jain MK, Singh VP (2005). DEM-based modelling of surface runoff using diffusion wave equation. J. Hydrol., 302(1-4): 107-126.

Jain MK, Kothyari UC, RangaRaju KG (2004). A GIS based distributed rainfall-runoff model. J. Hydrol., 299(1-2): 107-135.

Moore ID, Grayson RB (1991). Terrain-based catchment partitioning and runoff prediction using vector elevation data. Water Resour. Res., 27(6): 1177-1191.

Moore ID, Turner AK, Wilson JP, Jenson SK, Band LE (1993). GIS and land-surface-subsurface process modeling. Environ. modeling with GIS, pp. 196-230.

Muntohar AS, Liao HJ (2010). Rainfall infiltration: infinite slope model for landslides triggering by rainstorm. Natural Hazards, pp. 1-18.

Othman F, Naseri M (2011). Reservoir inflow forecasting using artificial neural network. Int. J. Phys. Sci., 6(3): 434-440.

Sepaskhah AR, Chitsaz H (2004). Validating the Green-Ampt Analysis of Wetted Radius and Depth in Trickle Irrigation. Biosys. Eng., 89(2): 231-236.

Smemoe CM (1999). The Spatial Computation of Sub-basin Green and Ampt Parameters.

Vieux BE (2004). Distributed hydrologic modeling using GIS. Kluwer Academic Publishers.

Watson FGR, Grayson RB, Vertessy RA, McMahon TA (1998). Large-scale distribution modelling and the utility of detailed ground data. Hydrol. Proc., 12(6): 873-888.

Wigmosta MS, Vail LW, Lettenmaier DP (1994).A distributed hydrology-vegetation model for complex terrain. Water Res. Res., 30(6): 1665-1680.